Network risk and forecasting power in phase-flipping dynamical networks

B. Podobnik,[1,2,3,4] A. Majdandzic,[1] C. Curme,[1] Z. Qiao,[5,6] W.-X. Zhou,[7] H. E. Stanley,[1] and B. Li[5,6,8]

[1]*Center for Polymer Studies and Department of Physics, Boston University, Boston, Massachusetts 02215, USA*

[2]*Faculty of Civil Engineering, University of Rijeka, 51000 Rijeka, Croatia*

[3]*Zagreb School of Economics and Management, 10000 Zagreb, Croatia*

[4]*Faculty of Economics, University of Ljubljana, 1000 Ljubljana, Slovenia*

[5]*NUS Graduate School for Integrative Sciences and Engineering, NUS, Singapore 117456, Singapore*

[6]*Department of Physics and Center for Computational Science and Engineering, NUS, Singapore 117546, Singapore*

[7]*School of Business, School of Science, and Research Center for Econophysics, East China University of Science and Technology, Shanghai 200237, China*

[8]*Center for Phononics and Thermal Energy Science, School of Physics Science and Engineering, Tongji University, Shanghai 200092, People's Republic of China*

(Received 2 December 2013; published 15 April 2014)

To model volatile real-world network behavior, we analyze a phase-flipping dynamical scale-free network in which nodes and links fail and recover. We investigate how stochasticity in a parameter governing the recovery process affects phase-flipping dynamics, and we find the probability that no more than $q\%$ of nodes and links fail. We derive higher moments of the fractions of active nodes and active links, $f_n(t)$ and $f_\ell(t)$, and we define two estimators to quantify the level of risk in a network. We find hysteresis in the correlations of $f_n(t)$ due to failures at the node level, and we derive conditional probabilities for phase-flipping in networks. We apply our model to economic and traffic networks.

DOI: 10.1103/PhysRevE.89.042807 PACS number(s): 89.75.Hc, 05.10.−a, 05.40.−a, 64.60.ah

I. INTRODUCTION

Across a broad range of human activities—from medicine, meteorology, and traffic management to intelligence services and military operations—forecasting theories help us estimate the probability of future outcomes. In general, the greater the uncertainty of the outcome, the more crucial it is that we be able to forecast future behavior. Since the nodes of many dynamic systems [1–22], such as traffic patterns and physiological networks, periodically fail and then recover—a disease spreads through an organism and then after a finite period of time the organism recovers—forecasting power [23–25] is highly relevant. It allows us to estimate the probability of future node and link failure and recovery and to quantify the level of risk in any given dynamic network.

When forecasting future node and link failure, we assume that networks are not static but time-dependent. The study of temporal networks has recently become one of the topics in network theory. It has been shown that many methods developed for static networks are inappropriate for the study of temporal (dynamic) networks [5,26–29] in which both nodes and links are active for only finite periods of time. For example, Ref. [6] defines a time-invariant function that characterizes the interactions of agents and constructs an activity-driven model that provides an explanation of structural features, such as the presence of hubs that emerge from the heterogeneous activity of agents. Reference [26] defines the average fraction of nodes in the sets of influence of all nodes as the reachability ratio. Reference [29] defines the temporal correlation coefficient and the temporal closeness centrality that quantify how quickly a node may on average reach other nodes in temporal networks.

Many models for temporal networks have been proposed [25,30–34]. References [30,31] propose social network models in which links represent such ephemeral social ties as face-to-face contacts. Reference [35] uses a null model that removes the timing correlations between the contact sequences of adjacent links, but keeps the temporal characteristics associated with the links. Reference [33] proposes a model for studying disease spreading in temporal networks. Reference [34] proposes a temporal network variant as an extension of the neighborhood vaccination scheme proposed in Ref. [18].

Reference [36] describes how the nodes in time-dependent regular networks and Erdös-Renyi networks (i) inherently fail, (ii) contiguously fail due to the failure of neighboring nodes, and (iii) recover. These networks exhibit phase-flipping between "active" and "inactive" collective network modes. Here we analyze networks with highly heterogeneous degree distributions, and we describe scale-free phase-flipping networks in which nodes and links fail and recover. We describe the collective behavior of these networks using two time-dependent network variables: the fraction of active nodes $f_n(t)$ and the fraction of active links $f_\ell(t)$. Our focus is on forecasting in dynamic networks. The goal is to calculate how many nodes will fail at any future time t, and thus to be able to quantify the risk in any given network.

II. MODEL

(i) At each time t any node in the system can independently fail, breaking its links with all other nodes, with a probability p. The internal failure state of node i we denote by spin $|S_i\rangle$ (if i is active, $|S_i\rangle = |1\rangle$).

(ii) The external failure states we denote by spin $|S_i'\rangle$, where $|S_i'\rangle$ is $|1\rangle$ if node i has more than $T_h\%$ active neighbors, and $|0\rangle$ (for a subsequent time $\tau' = 1$) with probability p_2 if $\leqslant T_h\%$ of i's neighbors are active. For scale-free networks, a percentage threshold T_h is the more appropriate choice than the constant T_h used in Ref. [36]. Node i—described by the two-spin state $|S_i, S_i'\rangle$—is active only if both spins are up (1), i.e., if $|S_i, S_i'\rangle = |1,1\rangle$.

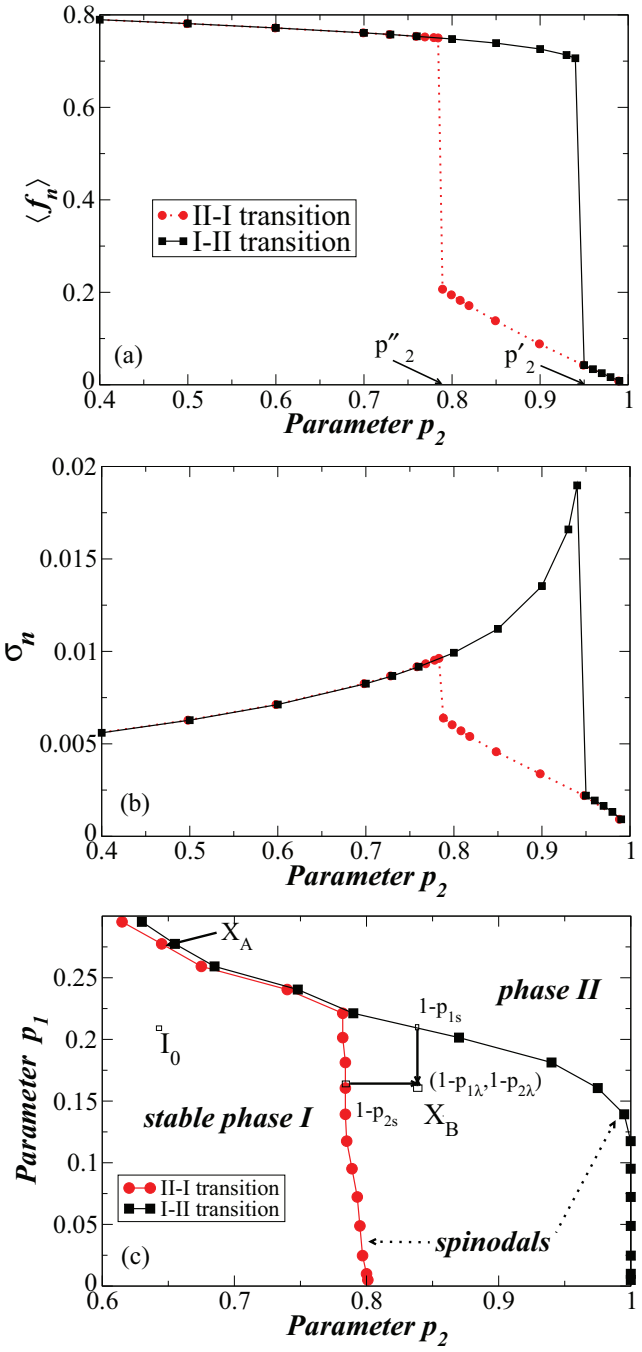

FIG. 1. (Color online) Network statistics used in analyzing (in)stability in the (i)–(iii) networks. In (a)–(c) we start with a BA network with $N = 10\,000$ and $\langle k \rangle = 3$, and then we introduce the (i)–(iii) network, where $T_h = 50\%$ and $\tau = 50$. Fixing p_1 and increasing p_2, for each (p_1, p_2) we calculate the fraction of active nodes, $f_n(t)$. We show hystereses for two network statistics: (a) the average $f_n(t)$, $\langle f_n \rangle$, and (b) the standard deviation of $f_n(t)$, σ_n. We use $p_1 = 0.2$ ($p = 0.004$) in two directions: from $p_2 = 0$ to 1, and then from $p_2 = 1$ to 0. As $p_2 \to p_2'$, $\langle f_n \rangle$ and σ_n exhibit first-order transitions. (c) Emergence of hysteresis in (p_1, p_2) space. The hysteresis point X_A is characterized by $\tau = 50$, $p = 0.0065$ ($p_1 = 0.277$), and $p_2 = 0.65$. The curves in (a)–(c) are the averages over different networks of the same fixed k. Different networks are characterized by different stochastic realizations and different choices for the initial nodes and links in BA networks.

(iii) After a time period τ, the nodes recover from internal failure. Usually τ is random, but we also analyze the case in which τ is constant [36].

Estimating how far the parameters of a dynamic system are from the area in parameter space characterized by high instability is crucial. For the network described in (i)–(iii) above, we arbitrarily choose parameters p_1 [related to p by $p_1 = 1 - \exp(-p\tau)$ [36]] and T_h. We then destabilize the network by increasing p_2, causing it to transition from phase I with predominantly active nodes to phase II with predominantly inactive nodes. In Fig. 1(a), for varying p_2, the first network statistic—the average $f_n(t)$, $\langle f_n \rangle$—gradually decreases for $p_2 \in (0, p_2')$ and then, at $p_2 \approx p_2'$, $\langle f_n \rangle$ shows a sudden network crash—a first-order phase transition. In Fig. 1(b) for $p_2 \in (0, p_2')$ the second network statistic—the standard deviation of $f_n(t)$, σ_n—becomes increasingly volatile. During network recovery, in Figs. 1(a) and 1(b) both $\langle f_n \rangle$ and σ_n follow a first-order phase transition, but at a value $p_2 = p_2''$, which differs from $(p_2 = p_2')$ obtained during the I–II transition. Because $\langle f_n \rangle$ and σ_n are dependent upon the initial node spins in the network, $p_2' \neq p_2''$ implies the existence of hysteresis [37–40]. To estimate the part of the (p_1, p_2) phase space that is unstable, we calculate the discontinuity (p_2', p_2'') values for varying p_1 values [see Fig. 1(b)]. Figure 1(c) shows a hysteresis with two discontinuity lines (spinodals) in the (p_1, p_2) space. The closer the (p_1, p_2) of a network is to the left spinodal in Fig. 1(c), the less stable is the network.

Reference [36] reports that introducing both a dynamic recovery with a (constant) parameter ($\tau \neq 0$) and a stochastic contiguous spreading ($p_2 \neq 1$) leads to spontaneous collective network phase-flipping phenomena. Figure 2 shows the fraction of active nodes $f_n(t)$ for constant τ ($\Delta\tau = 0$) that corresponds to the volatile state X_A shown in Fig. 1(c). Figure 2 shows that if τ is not constant but a random variable from a homogeneous probability distribution function (PDF), the phase-flipping phenomenon and thus the collective network mode disappear with increasing $\Delta\tau$ (increasing stochasticity in τ). Beginning with the relation $p_1 = 1 - \exp(-p\tau)$ [36] when τ is constant, we confirm this result. Suppose a network is initially set at a phase-flipping state X_A [Fig. 1(c)].

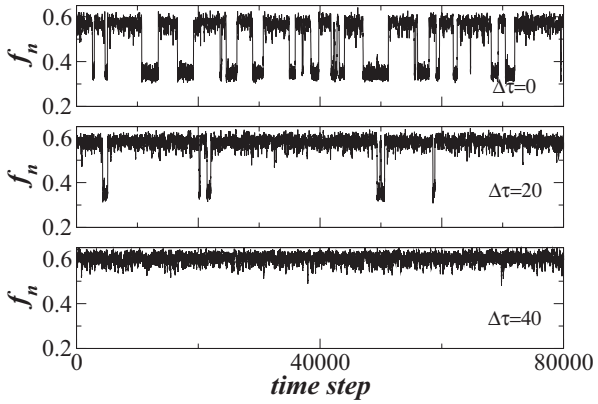

FIG. 2. Effect of stochasticity in τ on network phase-flipping. If τ is a random variable from a homogeneous PDF, $H(\tau_0 - \Delta\tau, \tau_0 + \Delta\tau)$, with $\tau_0 = 50$, the phase-flipping phenomenon gradually disappears with increasing $\Delta\tau$.

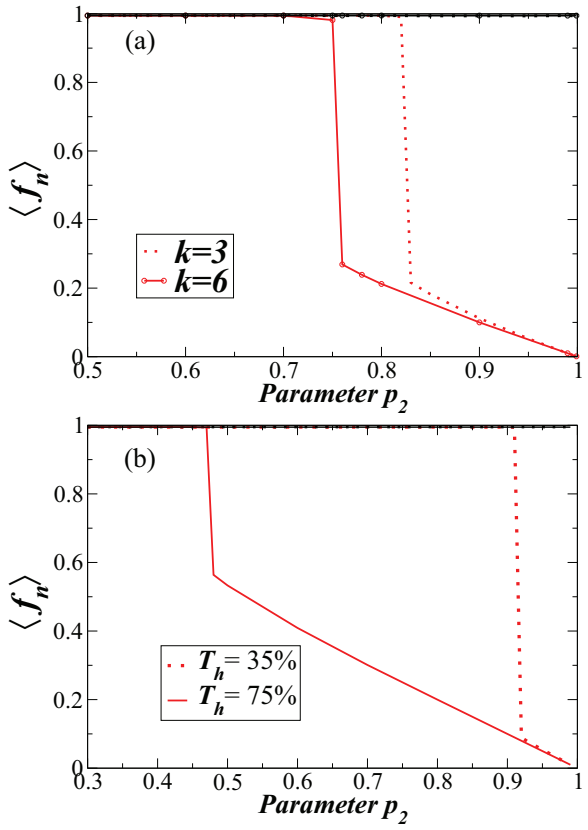

FIG. 3. (Color online) Dependence of hysteresis on parameters k and T_h%. Fixing p_1 and increasing p_2 for each (p_1,p_2), we calculate the fraction of active nodes, $f_n(t)$. (a) Average $f_n(t)$, $\langle f_n\rangle$ vs p_2 for $\langle k\rangle = 3$ and 6. With increasing $\langle k\rangle$, the hysteresis region is getting larger. We choose $T_h = 50\%$, $p = 0.0001$, and $\tau = 50$. (b) Average $f_n(t)$ vs p_2 for $T_h = 35\%$ and 75%. We set $p = 0.0001$, $\langle k\rangle = 6$, and $\tau = 50$. With increasing T_h, the hysteresis region is getting broader.

If τ follows a homogeneous PDF, $H(\tau_0 - \Delta\tau, \tau_0 + \Delta\tau)$, we easily derive the average parameter $p_1^* \equiv p_1(\Delta\tau)$ as

$$E(p_1^*) = 1 - \exp(-p\tau_0)\sinh(p\Delta\tau)/p\Delta\tau, \tag{1}$$

and the average deviation of p_1^* from $p_1 \equiv p_1(\Delta\tau = 0)$, $E(p_1^*) - p_1 = \exp(-p\tau_0)[1 - \sinh(p\Delta\tau)/p\Delta\tau] < 0$. With increasing $\Delta\tau$, $E(p_1^*) - p_1$ decreases and $E(p_1^*)$ moves from a volatile network regime (X_A) to a more stable network regime. Hence at X_A the less dispersed τ is (and also p_1), the more pronounced the phase-flipping. Hereafter, we analyze networks with constant τ.

Next we briefly analyze how parameters k and T_h affect the hysteresis curve. Figure 3(a) shows for two values of k that the hysteresis region grows as $\langle k\rangle$ increases. Similarly, Fig. 3(b) shows that the hysteresis region also grows as T_h increases.

III. NETWORK RISK

We next explore the diagnostic and forecasting power of dynamic networks. When internal (X) and external (Y) failures are independent, according to probability theory $P(X \cup Y) = P(X) + P(Y) - P(X)P(Y)$, from which Ref. [36] defines the probability $a = a(p,p_2,T_h) \equiv P(X \cup Y)$ that a randomly chosen node i is inactive,

$$a = p + p_2(1-p)\Sigma_k P(k)E(k,m,a), \tag{2}$$

equal to the fraction of inactive nodes, $a = 1 - \langle f_n\rangle$. Here $P(k)$ is the degree distribution, T_h, p, and p_2 are described in (i)–(ii) above, and $m \equiv T_h k$, $E(k,m,a) \equiv \Sigma_{j=0}^{m} a^{k-j}(1-a)^j \binom{k}{k-j}$ is the probability that the neighborhood of node i is critically damaged. Note that the internal failures affect the external failures, and therefore the above relation in Eq. (2) is only approximately true. As found in Ref. [36], the deviation of the mean-field approximation from simulations gradually decreases as degree k increases, which is a mean-field characteristic. For that reason, when a network is either small or moderately large, we calculate a numerically from a time series $f_n(t)$. For a network with N nodes, each with probability $(1-a)$ of being active, using a binomial distribution we obtain any moment of f_n of order q,

$$\langle f_n^q\rangle \equiv \Sigma_{j=0}^{N}\left(\frac{j}{N}\right)^q a^{N-j}(1-a)^j\binom{N}{j}, \tag{3}$$

that is, for large values of N, $\langle f_n^q\rangle \approx \int dx\, x^q G(x,\mu = 1-a,\sigma = \sqrt{a(1-a)/N})$—$G$ stands for Gaussian. The dependence of f_n^q on a explains why both $\langle f_n\rangle$ and σ_n in Fig. 1 show discontinuities for the same p_2 values.

We next quantify the level of stability of the (i)–(iii) network. Using the first two moments of Eq. (3), we define network risk (volatility) as $\sigma_n \equiv \sqrt{\langle f_n^2\rangle - (\langle f_n\rangle)^2}$. We define it this way because an absolutely stable network assumes that all nodes are active, $f_n(t) = 1$. With increasing network instability, the network $f_n(t)$ increasingly fluctuates over time, implying that the variance of $f_n(t)$ increases. In finance, the similar concept of stock price volatility is a measure of stock price variation over time [41]. Because a network is more stable when $f_n(t)$ is less volatile $(\sigma_n \to 0)$ and when $\langle f_n\rangle$ is as close to 1 as possible, we propose another network stability measure, namely the stability network ratio,

$$\langle f_n\rangle/\sigma_n, \tag{4}$$

where the larger the ratio is, the more stable is the network. Figure 4(a) shows that for a (i)–(iii) network, the ratio exhibits hysteresis behavior, e.g., with increasing instability $(p_2 \to 1)$, $\langle f_n\rangle/\sigma_n$ decreases. When N is large, $\langle f_n\rangle/\sigma_n = \sqrt{(1-a)N/a}$ [see Eq. (3)]. In practice, if two networks have equal $\langle f_n\rangle$ but different σ_n, the one with the larger ratio is the more stable. Note that a similar first-to-second moment of a price return is proposed in finance to quantify the performance of a financial asset [42]. Another signal-to-noise ratio defined as the ratio of mean to standard deviation of a signal is widely used in science and engineering [43].

IV. FORECASTING POWER IN DYNAMICAL NETWORKS

When we have an initial configuration of active nodes, we need to both estimate network volatility and determine how many nodes will have failed at any future time t. We allow the (i)–(iii) network in Fig. 1(c), initially at stable state I_0, to

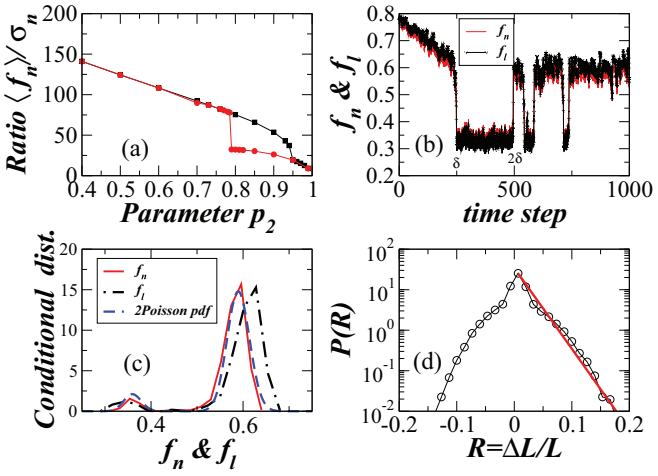

FIG. 4. (Color online) Network estimator and forecasting in the (i)–(iii) networks. (a) Network estimator, the ratio $\langle f_n \rangle / \sigma_n$, exhibits a strong hysteresis—the larger $\langle f_n \rangle / \sigma_n$, the more stable the network. The parameters used are as those in Fig. 1(a). The curve is the average over different networks. (b) The two fractions, f_n and f_ℓ, of the network with time-dependent p_1 that moves from I_0 [Fig. 1(c)] at time $t = 0$ to X_A during the first $\delta = 250$ steps. From δ to 2δ, the network stays in X_A. Upon reaching X_A, the network phase-flips between mainly "active," I, and mainly "inactive" phases, II. (c) Moving from I_0 to X_A after $t = 2\delta$, we calculate two CDFs, $C(f_n)$ and $C(f_\ell)$, both exhibiting a highly asymmetric bimodal shape. From $C(f_n)$ we can estimate the percentage of (in)active nodes at future t. Shown also is a combination of two Poissonian distributions, $w_1 P(\lambda_1) + w_1 P(\lambda_2)$, where $w_1 = 0.1$, $w_2 = 0.9$, $\lambda_1 = 0.59$, and $\lambda_2 = 0.36$, where λ_1 and λ_2 are $\langle f_n \rangle$ values in I and II. (d) For the number of active links, $L(t)$, we show $P[\Delta L(t)/L(t)]$ and its exponential fit.

move δ steps (with p_1 changing linearly) to a highly volatile phase-flipping state X_A. Figure 4(b) shows a representative $f_n(t)$. We always start from the same initial I_0, perform a large number of simulations [see Fig. 4(c)], and obtain the conditional distribution function (CDF), $C(f_n)$, from which we calculate the probability $[\int_{0.01q}^{1} C(f_n) df_n]$ that no more than $q\%$ nodes will be inactive at $t = 2\delta$. In finance, this probability approximates the risk that a substantial fraction of a financial system will collapse, the so-called "systemic risk" [44].

When we use f_n, we are assuming that every node is equally important. This frequently does not hold for real-world networks [2,3,45], e.g., when large banks become dysfunctional, they affect the overall financial network much more than dysfunctional small banks. In the (i)–(iii) network, the importance of each node is governed by network topology—the time-dependent node degree, $k(t)$. A randomly chosen link is active if both its nodes are active, and the probability that the link is active is $(1 - a)^2$. The average number of active links is

$$\langle L \rangle = (1 - a)^2 L_T, \tag{5}$$

where $L_T \equiv 1/2 \Sigma_{i=1}^{N} k_i$ denotes the total number of links when all links are active. Similar to Eq. (3) for a network with L_T links, each with probability $u \equiv (1 - a)^2$ of being active, a q-order moment of $f_\ell(t) = L(t)/L_T$—the fraction of active links—is

$$\langle f_\ell^q \rangle \equiv \Sigma_{j=0}^{L_T} \left(\frac{j}{L_T} \right)^q u^j (1 - u)^{L_T - j} \binom{L_T}{j}. \tag{6}$$

Figure 4(b) shows a representative $f_\ell(t)$, and Fig. 4(c) shows $C(f_\ell)$ [broader than $C(f_n)$] from which we can calculate the probability $[\int_{0.01q}^{1} C(f_\ell) df_\ell]$ that no more than $q\%$ of links will be inactive at t. Figure 4(d) shows the PDF of the relative change in $L(t)$ and its exponential fit—which is potentially important information for network management. Note that $\mathcal{L}(t) = L_T[1 - f_\ell(t)]$ denotes the loss of a network's links. Using Eq. (5), we obtain $\langle \mathcal{L} \rangle \equiv L_T - \langle L \rangle = a(2 - a) L_T$.

The (i)–(iii) network model exhibits one more potentially important forecasting property. Suppose a network set in a state X_B [see Fig. 1(c)] within the hysteresis regime is predominantly inactive. Reference [36] defines a local time-dependent parameter $p_{2,\lambda}(t) = \frac{1}{\lambda} \Sigma_{i=1}^{\lambda} p_2(t + 1 - i)$ as the average fraction of externally failed nodes over the most recent interval of length λ. When $p_{2,\lambda}(t)$ crosses the "left" spinodal, the network shifts from the inactive phase II to the active phase I. Similarly, $p_{1,\lambda}(t) = \frac{1}{\lambda} \Sigma_{i=1}^{\lambda} p_1(t + 1 - i)$. In Ref. [36], the PDF of $p_{2,\lambda}(t)$ $[p_{1,\lambda}(t)]$ determines the average lifetime of the system in I and II. Here we find that $p_2(t)$ follows a binomial distribution that can be approximated for large samples n with the normal distribution $N(\mu = p_2, \sigma^2 = p_2(1 - p_2)/n) \equiv P[p_2(t)] \sim \exp[-\frac{n[p_2(t) - p_2]^2}{2p_2(1 - p_2)}]$, where $n = NE(a(p_1, p_2), k, m)$ [see Eq. (2)]. From $p_{2,\lambda}(t) = \frac{1}{\lambda} \Sigma_{i=1}^{\lambda} p_{2,t+1-i}$, we easily derive $p_{2,\lambda}(t) = p_2(t)/\lambda + p_{2,\lambda}(t - 1) - p_2(t - \lambda)/\lambda$.

Thus, having information about the previous $p_{2,\lambda}$, $p_{2,\lambda}(t - 1)$, we can forecast the current value, where the closer $p_{2,\lambda}$ is to a spinodal, the larger the probability that the phase will flip. We quantify this probability using the CDF

$$C[p_{2,\lambda}(t)] \sim \exp\left[-\frac{N\lambda^2 E(a(p_1, p_2), k, m)[p_{2,\lambda}(t) - p_{2\lambda}(t - 1) + p_2(t - \lambda)/\lambda - p_2/\lambda]^2}{2p_2(1 - p_2)} \right]. \tag{7}$$

This probability can be used to estimate, given the most recent local state $p_{2\lambda}(t - 1)$ and $p_2(t - \lambda)$, the probability $P(x \leqslant p_{2s} | p_{2\lambda}(t - 1), p_2(t - \lambda))$ that the network will move from being predominantly inactive, II, to predominantly active, I—here, as in Ref. [36], p_{2s} is a spinodal value where the network phase-flips from II to I [Fig. 1(c)]. Similarly, if p_{1s} defines a spinodal value at which the network phase-flips from phase I to II [Fig. 1(c)], from the CDF,

$$C[p_{1\lambda}(t)] \sim \exp\left[-\frac{N\lambda^2 [p_{1,\lambda}(t) - p_{1\lambda}(t - 1) + p_1(t - \lambda)/\lambda - p_1/\lambda]^2}{2p_1(1 - p_1)} \right], \tag{8}$$

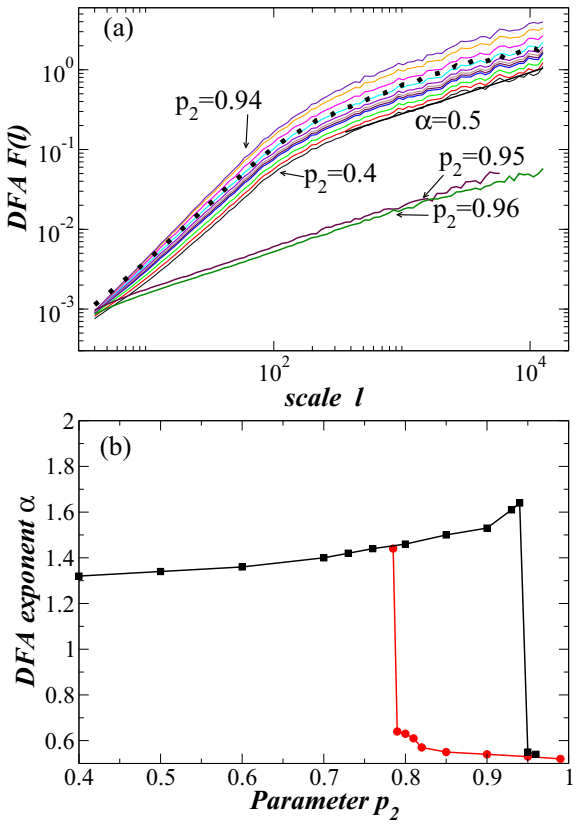

FIG. 5. (Color online) Emergence of correlations at the network level due to failure at the node level. (a) For each time series (constant p_2) used in Fig. 1(a), we show the DFA plot of $f_n(t)$ vs scale ℓ, $F(\ell) \propto (\ell)^{\alpha}$, for the I-II transition. With increasing p_2 up to 0.94, $F(\ell)$ moves upward, accompanied by a small (b) increase in the DFA exponent α. α exhibits a crossover at a scale l that varies with the recovery times τ and τ'. Suddenly, at $p_2 \approx 0.94$, the DFA exponent drops in a first-order phase transition. We also show correlations in the fraction of externally failed nodes (dotted lines), responsible for correlations in f_n. (b) Exponent α, calculated for both I-II and II-I transitions for scales $\ell \leqslant 100$, exhibits a clear hysteresis. The curve is the average over different networks.

we can estimate the probability $P(x \geqslant p_{1s}|p_{1\lambda}(t-1), p_1(t-\lambda))$ that the network will fall into the predominantly inactive phase (e.g., as in an economic recession) within the next period.

In short, we can forecast the future behavior of a dynamic network by calculating (a) the probability that no more than q% nodes will be inactive at any future time t, and (b) the probability that a network will move from being predominantly inactive, II, to predominantly active, I, and vice versa.

V. TEMPORAL CORRELATIONS IN DYNAMICAL NETWORKS

Finally we examine the emerging hysteresis in the correlations of $f_n(t)$ due to network dysfunctionality at the node level. For each time series $f_n(t)$ ($\tau = \text{const}$) in Figs. 1(a) and 1(b) we apply detrended fluctuation analysis (DFA) [46]—$F^2(l) \propto l^{2\alpha}$. Figure 5(a) shows that $f_n(t)$ exhibits finite-range correlations of the random-walk type ($\alpha \approx 1.5$) with a clear first-order phase transition in which a sudden change in the correlation exponent α occurs when p_2 approaches the value at which we expect network collapse (see Fig. 1). An approximate explanation of the correlations in $f_n(t)$ is that correlations in $f_n(t)$ and its hysteresis behavior are due to correlations in the fractions of externally failed nodes $p_2(t)$ and internally failed nodes $p_1(t)$. Figure 5(a) confirms this assumption by showing only correlations in $p_2(t)$. The existence of hysteresis [38–40] in Fig. 5(b) indicates that the correlations in collective modes are not the same when the network approaches network collapse and when the network recovers—if, e.g., our network models the global economy, then when the economy moves from "bad" to "good" years, "good" years are never as good as the previous "good" years.

VI. DATA ANALYSIS

To demonstrate how our model describes an economic network in which firms are treated as nodes, we connect our model parameters p, τ, and T_h to real financial variables. Since the seminal paper of Ref. [47], many models have been developed in finance to estimate the probability p_f that a firm will experience financial distress. This probability is only partially related to the (i) probability of internal failure p because p does not take into account the possibility that the firm may fail because of the proximity of failed neighbors. Using the the second parameter τ, we define the period of time needed for an internally failed node to recover. The counterpart to parameter τ in finance is the average time a firm experiences financial distress, which in the United States is approximately two years [48]. We relate the third parameter T_h—the vulnerability—to finance by first recognizing that a bank i has a set of financial variables, e.g., interbank assets $A_{B,i}$, interbank liabilities $L_{B,i}$, deposits D_i, and illiquid assets $A_{M,i}$ [49]. We define solvency in a bank as $(1-\phi)A_{B,i} + A_{M,i} - L_{B,i} - D_i > 0$, where ϕ denotes the fraction of neighbor banks to i that have failed [49]. In addition, the larger the bank's capital buffer $K_i = A_{B,i} + A_{M,i} - L_{B,i} - D_i$, the less the bank will depend on its neighbors. Thus in our model K_i is inversely related to T_h [50].

To demonstrate the utility of the (i)–(iii) network model when analyzing real-world networks, we first analyze a small economic network of 19 developed countries [51], and we use an output measurement of trading dynamics, *per capita* gross domestic product—GDP. For each country and for each year t between 1870 and 2012 [52], a country (node) is active if the GDP growth is non-negative (if it has been a "good" year). Figure 6(a) shows the fraction of active countries $f_n(t)$ that are becoming increasingly interdependent due to globalization [the nonstationarity analyzed in Fig. 4(b)]. When we disregard this nonstationarity, we find model parameters ($p = 0.082 \pm 0.02$, $p_2 = 0.77 \pm 0.03$, $\tau = 1.33 \pm 0.5$, and $T_h = 56 \pm 3\%$) for which the $\langle f_n \rangle$ of our model and the second network moment σ_n are the best fits of the empirical moments. Figure 6(b) shows the $f_n(t)$ of the model. From $p_1 = 1 - \exp(-p\tau)$ [36], $p_1 = 0.103$ suggests that any randomly chosen developed country will experience recession (failure) approximately every ten years, since p_1 represents the average fraction of internally failed nodes [36]. The parameter $p_2 = 0.77$ indicates that there is an $\approx$77% probability that a country

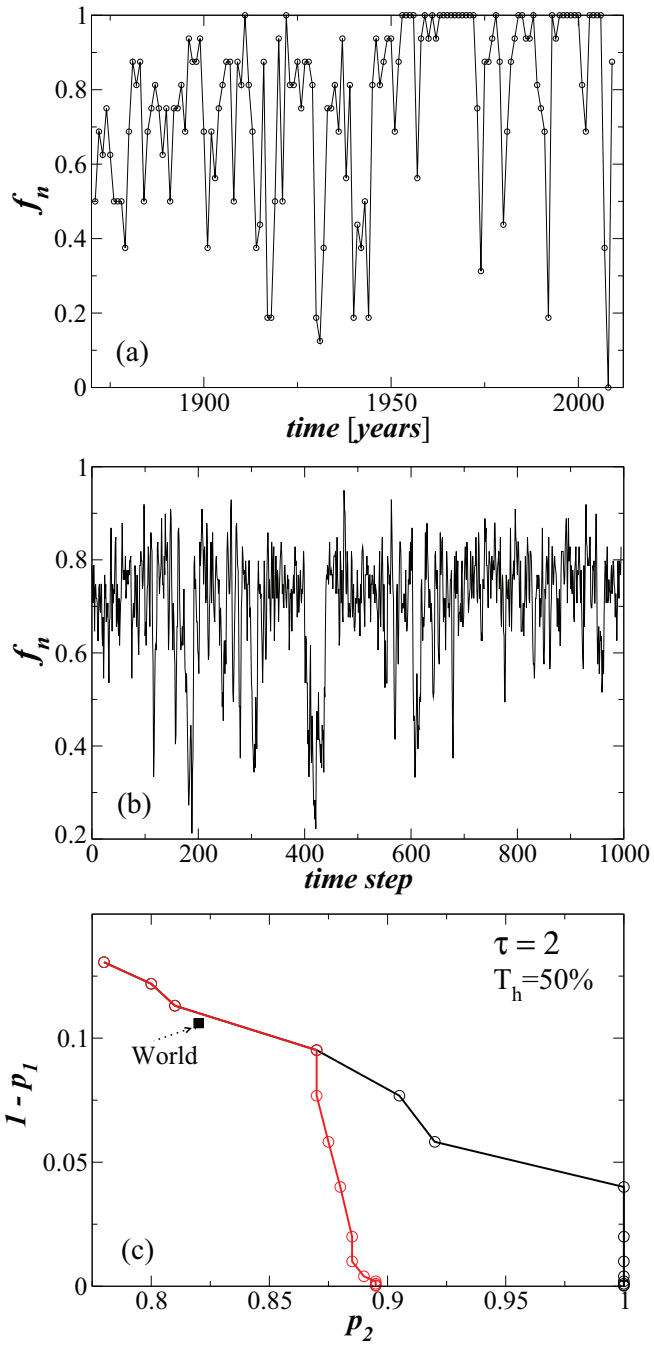

FIG. 6. (Color online) Application of dynamical networks. (a) Economics—how far is an economy from a volatile regime? Fraction of developed countries, $f_n(t)$, not in recession ($\Delta gdp > 0$). (b) For a (i)–(iii) network we show the model's $f_n(t)$ obtained by fitting the first and the second moments in (a), where $\tau = 1.3$, $T_h = 56\%$, $p_1 = 0.103$, and $p_2 = 0.77$. (c) Hysteresis with two spinodals for the (i)–(iii) network with $N = 100$, $\tau = 2$, and $T_h = 50\%$. The parameter set is close to the critical line in the supercritical region.

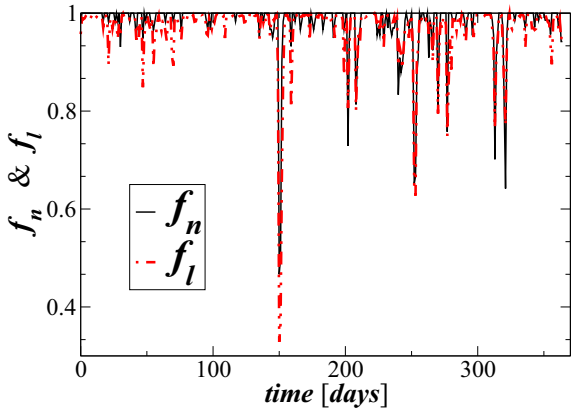

FIG. 7. (Color online) Air traffic network. Fraction of active northeastern US airports, f_n, with more than 40% of canceled flights. We also show f_ℓ.

will undergo recession if its trading partners have recently experienced recession. Figure 6(c) shows the hysteresis [38] in (p_1, p_2) space for the (i)–(iii) network model with $\tau = 2$ and $T_h = 50\%$. We also show developed countries with $p_1 = 0.106 \pm 0.01$, $p_2 = 0.82 \pm 0.02$. We next analyze $f_n(t)$ for 23 Latin American countries, 25 EU countries, and 25 Asian countries for each year since 1980. We calculate the network stability ratio $\langle f_n \rangle / \sigma_n$ of Eq. (4) for each group and obtain the values 3.25, 4.15, and 6.95.

We next analyze the airport traffic network [53] in the northeastern United States (The Library of Congress definition) comprising 66 airports (nodes), and we consider only those flights (links) within the northeast. For each day during the period from June 1, 2012 to May 31, 2013, we calculate the fraction of failed airports, $1 - f_n(t)$. We arbitrarily define failed airports as those in which more than $T_h = 40\%$ flights have been canceled for the day. The air traffic network in Fig. 7, as expected, shows a much higher level of node stability than is typical in economic networks—i.e., rarely does $1 - f_n(t)$ reach 40%. Since the air traffic network is scale-free [23], we apply the (i)–(iii) network model to fit the empirical $\langle f_n \rangle$ and σ_n data to the parameters of the model—$p = 0.011 \pm 0.003$ and $p_2 = 0.92 \pm 0.03$. Note that airports in the air traffic network still function when links fail (when flights are canceled). This suggests that an item (iv) could be added to the (i)–(iii) dynamic network model, namely the failure probability, p_3, of each link.

ACKNOWLEDGMENTS

B.P. thanks the ZSEM (Grant No. ZSEM08007) for support. This work is also partially supported by an NUS Grant "Econophysics and Complex Networks" (R-144-000-313-133). The BU work is supported by the Keck Foundation, ONR (Grant No. N00014-09-1-0380, Grant No. N00014-12-1-0548), DTRA (Grant No. HDTRA-1-10-1-0014, Grant No. HDTRA-1-09-1-0035), and NSF (Grant No. CMMI 1125290). W.X.Z. received financial support from NSFC (Grant No. 11075054).

[1] D. J. Watts and S. H. Strogatz, Nature (London) **393**, 440 (1998).

[2] R. Albert and A.-L. Barabási, Rev. Mod. Phys. **74**, 47 (2002).

[3] S. N. Dorogotsev and A. V. Goltsev, Rev. Mod. Phys. **80**, 1275 (2008).
[4] M. E. J. Newman, *Networks: An Introduction* (Oxford University Press, New York, 2010).
[5] P. Holme and J. Saramaki, Phys. Rep. **519**, 97 (2012).
[6] N. Perra, B. Goncalves, R. Pastor-Satorras, and A. Vespignani, Sci. Rep. **2**, 469 (2012).
[7] A.-L. Barabási and R. Albert, Science **286**, 509 (1999).
[8] S. N. Dorogovtsev, J. F. F. Mendes, and A. N. Samukhin, Phys. Rev. Lett. **85**, 4633 (2000).
[9] P. L. Krapivsky, S. Redner, and F. Leyvraz, Phys. Rev. Lett. **85**, 4629 (2000).
[10] A. Krawiecki, J. A. Holyst, and D. Helbing, Phys. Rev. Lett. **89**, 158701 (2002).
[11] R. Pastor-Satorras and A. Vespignani, Phys. Rev. Lett. **86**, 3200 (2001).
[12] L. Adamic and B. A. Huberman, Nature (London) **401**, 131 (1999).
[13] R. Albert, H. Jeong, and A.-L. Barabási, Nature (London) **406**, 378 (2000).
[14] R. Milo *et al*., Science **298**, 824 (2002).
[15] S. Jain and S. Krishna, Phys. Rev. E **65**, 026103 (2002).
[16] D. Garlaschelli, G. Caldarelli, and L. Pietronero, Nature (London) **423**, 165 (2003).
[17] S. V. Buldyrev *et al*., Nature (London) **464**, 1025 (2010).
[18] R. Cohen, K. Erez, D. ben-Avraham, and S. Havlin, Phys. Rev. Lett. **85**, 4626 (2000).
[19] R. Parshani, S. V. Buldyrev, and S. Havlin, Proc. Natl. Acad. Sci. (USA) **108**, 1007 (2011).
[20] N. Perra, A. Baronchelli, D. Mocanu, B. Goncalves, R. Pastor-Satorras, and A. Vespignani, Phys. Rev. Lett. **109**, 238701 (2012).
[21] J. Gao, S. V. Buldyrev, H. E. Stanley, and S. Havlin, Nat. Phys. **8**, 40 (2012).
[22] B. Podobnik, M. Dickison, D. Horvatic, and H. E. Stanley, Europhys. Lett. **100**, 50004 (2012).
[23] V. Colizza, A. Barrat, M. Barthelemy, and A. Vespignani, Proc. Natl. Acad. Sci. (USA) **103**, 2015 (2005).
[24] A. Vespignani, Science **325**, 425 (2009).
[25] M. Kolar, L. Song, A. Ahmed, and E. P. Xing, Ann. Appl. Stat. **4**, 94 (2010).
[26] P. Holme, Phys. Rev. E **71**, 046119 (2005).
[27] R. K. Pan and J. Saramaki, Phys. Rev. E **84**, 016105 (2011).
[28] J. Moody, Social Forces **81**, 25 (2002).
[29] J. Tang, S. Scellato, M. Musolesi, C. Mascolo, and V. Latora, Phys. Rev. E **81**, 055101 (2010).
[30] J. Stehle, A. Barrat, and G. Bianconi, Phys. Rev. E **81**, 035101 (2010).
[31] K. Zhao, J. Stehle, G. Bianconi, and A. Barrat, Phys. Rev. E **83**, 056109 (2011).
[32] H. H. Jo, R. K. Pan, and K. Kaski, PLoS ONE **6**, e22687 (2011).
[33] C. Kamp, PLoS Comp. Biol. **6**, e1000984 (2010).
[34] S. Lee, L-E. C. Rocha, F. Liljeros, and P. Holme, PLoS ONE **7**, e36439 (2012).
[35] M. Karsai, M. Kivelä, R. K. Pan, K. Kaski, J. Kertész, A.-L. Barabási, and J. Saramäki, Phys. Rev. E **83**, 025102(R) (2011).
[36] A. Majdandzic *et al*., Nat. Phys. **10**, 34 (2014).
[37] T. A. Kesselring *et al*., Sci. Rep. **2**, 474 (2012).
[38] O. J. Blanchard and L. H. Summers, Eur. Econ. Rev. **31**, 288 (1987).
[39] D. Angeli, J. E. Jr. Ferrell, and E. D. Sontag, Proc. Natl. Acad. Sci. (USA) **17**, 1822 (2004).
[40] J. Das *et al*., Cell **136**, 337 (2009).
[41] R. Roll, J. Finance **39**, 1127 (1984).
[42] W. F. Sharpe, J. Business **39**, 119 (1966).
[43] J. T. Bushberg *et al*., *The Essential Physics of Medical Imaging* (Lippincott Williams & Wilkins, Philadelphia, 2006).
[44] D. Bisias, M. Flood, A. W. Lo, and S. Valavanis, Annual Review of Financial Economics **4**, 255 (2012).
[45] W. Miura, H. Takayasu, and M. Takayasu, Phys. Rev. Lett. **108**, 168701 (2012).
[46] C. K. Peng, S. V. Buldyrev, S. Havlin, M. Simons, H. E. Stanley, and A. L. Goldberger, Phys. Rev. E **49**, 1685 (1994).
[47] E. Altman, J. Finance **23**, 589 (1968).
[48] A. C. Eberhart, W. T. Moore, and R. L. Roenfeldt, J. Finance **45**, 1457 (1990).
[49] P. Gai and S. Kapadi, Proc. R. Soc. A **466**, 2401 (2010).
[50] B. Podobnik *et al*., arXiv:1403.5623.
[51] The dataset includes 15 EU countries, the United States, Australia, New Zealand, and Canada.
[52] http://www.ggdc.net/maddison/maddison-project/home.htm.
[53] http://www.rita.dot.gov/bts/.